
NEORL: NeuroEvolution Optimization with Reinforcement Learning

Majdi I. Radaideh*

Department of Nuclear Science and Engineering,
Massachusetts Institute of Technology,
Cambridge, MA 02139, United States
radaideh@mit.edu

Katelin Du*

Department of Nuclear Science and Engineering,
Massachusetts Institute of Technology,
Cambridge, MA 02139, United States

Paul Seurin*

Department of Nuclear Science and Engineering,
Massachusetts Institute of Technology,
Cambridge, MA 02139, United States

Devin Seyler

Department of Physics,
Massachusetts Institute of Technology,
Cambridge, MA 02142, United States

Xubo Gu

School of Nuclear Science and Engineering,
Shanghai Jiao Tong University,
Shanghai 200240, China

Haijia Wang

Department of Electrical Engineering and Computer Science,
Massachusetts Institute of Technology,
Cambridge, MA 02142, United States

Koroush Shirvan

Department of Nuclear Science and Engineering,
Massachusetts Institute of Technology,
Cambridge, MA 02139, United States

ABSTRACT

We present an open-source Python framework for NeuroEvolution Optimization with Reinforcement Learning (NEORL) developed at the Massachusetts Institute of Technology. NEORL offers a global optimization interface of state-of-the-art algorithms in the field of evolutionary computation, neural networks through reinforcement learning, and hybrid neuroevolution algorithms. NEORL features diverse set of algorithms, user-friendly interface, parallel computing support, automatic hyperparameter tuning, detailed documentation, and demonstration of applications in mathematical and real-world engineering optimization. NEORL encompasses various optimization problems from combinatorial, continuous, mixed discrete/continuous, to high-dimensional, expensive, and constrained engineering optimization. NEORL is tested in variety of engineering applications relevant to low carbon energy research in addressing solutions to climate change. The examples include nuclear reactor control and fuel cell power production. The results demonstrate NEORL competitiveness against other algorithms and optimization frameworks in the literature, and a potential tool to solve large-scale optimization problems. More examples and benchmarking of NEORL can be found here: <https://neorl.readthedocs.io/en/latest/index.html>

Keywords Optimization · Deep Reinforcement Learning · Evolutionary Computation · Neuroevolution · Nuclear Reactor Design, Carbon-free energy

*Review in Progress * Authors with equal contribution

1 Introduction

Optimization refers to the process of finding the best possible solution(s) such that an objective function is met. As the real-world engineering designs grow in complexity, the needs for new optimization techniques and friendly frameworks to implement them become more needed than before. In recent decades, global optimization techniques have been extensively applied to various domains, including but not limited to engineering [1, 2], machine learning [3], finance [4], health care [5], and many others. In this literature review, we classify optimization algorithms into four major categories relevant to our proposed research: evolutionary algorithms (EA), neural-based algorithms, hybrid neuroevolution, and gradient-based algorithms.

Genetic algorithms (GA) [6] are undoubtedly the face and origin of a long chain of metaheuristics and EAs. GA, which evolve population using natural operators (e.g. crossover, mutation, selection), inspired a set of algorithms called “evolution strategies” (ES). ES are effective for continuous optimization [7, 8] and have been used as an alternative to gradient descent to train neural networks [9]. Following GA footprints, a set of classical evolutionary and swarm algorithms has been developed including particle swarm optimization (PSO) [10], differential evolution (DE) [11], ant colony optimizer (ACO) [12], and tabu search (TS) [13], which dominated the field until the late 1990s. During the early 2000s, new EA started to emerge such as artificial bee colony (ABC) [14], cuckoo search (CS) [15], and bat algorithm (BAT) [16]. In the past 10 years, the development of EA has become more nature-inspired. The main modern EAs that show promise and popularity are: grey wolf optimizer (GWO) [17], whale optimization algorithm (WOA) [18], moth-flame optimization (MFO) [19], salp swarm algorithm (SSA) [20], and recently the Harris hawks optimizer (HHO) [21]. An overview of classical EA and evolution strategies can be found here [22], while modern EAs and their applications are reviewed here [23, 24]. Implementation-wise in Python, DEAP [25] provides a solid framework for classical EA such as GA, genetic programming, and evolution strategies, while EvoloPy [26] provides an implementation of modern EA such as GWO, HHO, WOA, and MFO along with some basic implementation of classical GA and PSO.

Although neural networks are probably older than EA, they started to emerge back in the mainstream when more computing power and data became available [27]. Artificial neural networks trained by supervised learning demonstrated some success in solving global optimization problems [28, 29], even though their practical implementation always faces major challenges. The dimensionality of the search space and the “dynamic” nature of the optimization problem are restrictions for generating a representative labeled training data for the neural networks. Therefore, in this work, we focus on a certain class of neural network algorithms trained by reinforcement learning (RL) [30]. What makes RL special for optimization is that it does not require a pre-generated labeled data (like unsupervised or supervised learning). Alternatively, the agent collects features and labels as needed, guided by a reward signal (e.g. fitness value) to meet a certain reward value. This analogy seems ideal for optimization, as the agent can adapt to the search region to learn to generate individuals that maximize/minimize a certain objective function, which acts as the reward signal. This inspiration has led to the term “learning to optimize” [31], which has been followed by many attempts to use RL and neural networks to solve optimization problems. See for example [32] on using RL with recurrent neural network policy for combinatorial optimization, or [33] for using graph embedding and RL to solve combinatorial optimization over graphs, or [34] for using deep Q learning and proximal policy optimization for physics-informed optimization of nuclear fuel. A comprehensive overview of using machine learning and neural networks to solve combinatorial optimization is conducted by [35]. To our knowledge, currently, there is no framework providing generic implementation of neural networks and RL for optimization purposes. However, OpenAI baselines [36] and stable-baselines [37] provided an implementation of the state-of-the-art RL algorithms for applications on game-playing AI and autonomous control. These frameworks provided a solid base for us as we have built on their implementation to leverage our RL and neural optimizers.

The field of neuroevolution started to grow simultaneously as the neural and evolutionary fields do to obtain the best of both worlds. Neuroevolution augmenting topologies (NEAT) [38] and its modified version, hypercube-based NEAT (HyperNEAT) [39] are probably the most common in this area. In these hybrid algorithms, GA is used to evolve neural network topologies by using evolutionary operators to optimize network width, depth, weights, biases, and activation. NEAT has inspired other researchers to transfer neuroevolution to train deep neural networks and RL systems as shown by these GA and deep neuroevolution efforts [40] or as shown by using PSO [41, 42]. Neuroevolution can contribute to the field of optimization in two major forms. The first form is *exchanging solutions between evolutionary and neural algorithms during search* to help increasing search diversity, improving solution quality, and accelerate convergence. Hybrid neuroevolution optimizers have been developed in the literature, for example, GA crossover and mutation have been controlled by Q-learning [43], and RL algorithms have been used to inform and guide EA search in constrained optimization [44]. Furthermore, EA are used as an alternative to temporal credit assignment and value function in RL [45]. A comprehensive overview of RL, EA, and the history of their hybridization can be found in this review [46]. The second form is through *using neural networks as surrogates to assist EA*. Although supervised neural networks

have limited scope in tackling the optimization problem directly, supervised networks excelled as surrogate models to assist EA in tackling expensive fitness functions [47]. A class of hybrid neuroevolution algorithms involves using EA to optimize the problem, while neural networks are trained based on evolutionary-generated data to approximate the original fitness function [48]. For example, feedforward [49] and Bayesian [50] neural network surrogates were used to assist EA in optimizing expensive functions. To our knowledge, currently, there is also no framework providing generic implementation of neuroevolution for optimization purposes either as an optimizer or as a hybrid surrogate algorithm.

Lastly, gradient-based or deterministic optimization algorithms exist in the literature and have been used for decades. This optimization category offers fast search and convergence, but suffers from major issues such as local optima entrapment, requirement of derivation (i.e. closed-form fitness function is needed), and computational limitations to calculate the derivatives of high-dimensional problems. Indeed, these limitations encourage the development of the prescribed three optimization categories (neural, evolutionary, neuroevolution). Fortunately, gradient-based algorithms are well-implemented and tested. For example, `nlopt` [51], `PyOpt` [52], and `scipy.optimize` [53] are just few examples of robust Python implementation of popular algorithms such as BFGS, Newton-Conjugate-Gradient, Sequential Least Squares Programming (SLSQP), Method of Moving Asymptotes, Preconditioned truncated Newton, and a variety of trust-region-based methods. Given that gradient-based algorithms are mature enough with solid literature implementation, this category is not discussed further here.

In this work, we propose NEORL (NeuroEvolution Optimization with Reinforcement Learning) as a new open-source Python framework that brings the latest developments of machine learning and evolutionary computation to serve the optimization research community, including energy and engineering applications. The novelty and uniqueness of NEORL compared to other optimization frameworks can be summarised as follows:

- NEORL offer a diverse set of +25 algorithms that belong to evolutionary computation, neural networks, and neuroevolution categories. The diversity of the implemented algorithms allow the user to test different types of algorithms on the same problem; obtaining a more comprehensive understanding and better results.
- NEORL includes efficient implementation of previously proposed algorithms. It also includes new algorithms proposed and developed by the authors themselves such as RL-informed evolutionary algorithms, EA with prioritized experience replay, and neural Harris hawks optimizer.
- NEORL supports discrete, categorical, and continuous search spaces as well as mixed discrete-categorical-continuous optimization. We demonstrate how to use NEORL to solve the combinatorial travelling salesman problem, mixed-integer optimization, and pure continuous engineering optimization.
- NEORL supports parallel computing. Vast majority of NEORL algorithms offer parallel optimization to accelerate the optimization of expensive fitness functions, which can be simply activated by a flag. This highlights a major advantage of NEORL over other frameworks for large-scale expensive problems.
- NEORL supports internal hyperparameter tuning. NEORL offers automatic search to tune the optimizer hyperparameters to maximize its performance. Some algorithms, especially neural-based, have multiple hyperparameters to tune. The user can choose between grid search, random search, evolutionary search, or Bayesian search for that purpose.
- NEORL is fully documented with a variety of unit tests, benchmarks, and engineering examples, which enable a friendly user experience.

For the remaining sections of this work, the optimization methodology of major NEORL algorithms are described in section 2. In section 3, NEORL structure is presented, which includes a step-by-step procedure to construct a complete NEORL problem, and a comparison with existing frameworks. Section 4 presents NEORL application to variety of energy optimization problems that belong to nuclear power and fuel cell energy production. The reader can also find additional applications of NEORL in the webpage². Discussions and conclusions of this work are highlighted in section 5.

²<https://neorl.readthedocs.io/en/latest/index.html>

2 Optimization Methodology

Without loss of generality, the standard form of a minimization optimization problem can be formulated as:

$$\begin{aligned}
 & \min_{\vec{x}} f(\vec{x}), \\
 & \text{subject to,} \\
 & g_i(\vec{x}) \geq 0, \quad i = 1, 2, \dots, m, \\
 & h_j(\vec{x}) = 0, \quad j = 1, 2, \dots, p,
 \end{aligned} \tag{1}$$

where f is the objective function to be minimized over the input vector \vec{x} , which has a size d . $g_i(\vec{x}) \leq 0$ are inequality constraints with a total of m constraints, $h_j(\vec{x}) = 0$ are equality constraints with a total of p constraints. When $p = 0$ and $m = 0$, the problem becomes unconstrained. The maximization problem can be formulated similarly by optimizing the negative form of the objective function f .

The discrete/combinatorial optimization problem formulation is similar to Eq.(1), except that the values of \vec{x} are restricted to discrete values (e.g. 1, 2, 3, ...). For the mixed discrete-continuous problems, the variable types in \vec{x} can be different, e.g. x_1 is a continuous variable, x_2 is discrete, and so on.

A summary of all supported optimization algorithms in NEORL is provided in Table 1, which includes their multiprocessing and input space support. In the next subsections, we discuss three different algorithm categories, which NEORL algorithms belong to.

Table 1: List of NEORL algorithms and their optimization support

Num.	Algorithm	Category	Discrete Space	Continuous Space	Mixed Space	Multiprocessing
1	PPO	Neural	✓	✓	✓	✓
2	A2C	Neural	✓	✓	✓	✓
3	DQN	Neural	✓	×	×	×
4	ACKTR	Neural	✓	✓	✓	✓
5	ACER	Neural	✓	×	×	✓
6	ES/GA	Evolutionary	✓	✓	✓	✓
7	PSO	Evolutionary	✓	✓	✓	✓
8	DE	Evolutionary	✓	✓	✓	✓
9	XNES	Evolutionary	×	✓	×	✓
10	GWO	Evolutionary	✓	✓	✓	✓
11	PESA	Hybrid	✓	✓	✓	✓
12	PESA2	Hybrid	✓	✓	✓	✓
13	SA	Evolutionary*	✓	✓	✓	✓
14	SSA	Evolutionary	✓	✓	✓	✓
15	WOA	Evolutionary	✓	✓	✓	✓
16	HHO	Evolutionary	✓	✓	✓	✓
17	MFO	Evolutionary	✓	✓	✓	✓
18	JAYA	Evolutionary	✓	✓	✓	✓
19	BAT	Evolutionary	✓	✓	✓	✓
20	RNEAT	Hybrid	×	✓	×	✓
21	FNEAT	Hybrid	×	✓	×	✓
22	ACO	Evolutionary	×	✓	×	✓
23	PPO-ES	Hybrid	✓	✓	✓	✓
24	ACKTR-DE	Hybrid	✓	✓	✓	✓
25	NHHO	Hybrid	✓	✓	✓	✓
26	NGA	Hybrid	×	✓	×	×
27	CS	Evolutionary	✓	✓	✓	✓
28	TS	Evolutionary	✓	×	×	×

* Simulated Annealing (SA) does not belong directly to evolutionary algorithms, but to a more generic category of stochastic optimization

2.1 Evolutionary Algorithms

Also known as metaheuristics, EA in NEORL form a basis for direct optimization and also as a baseline to leverage hybrid neuroevolution algorithms. Almost all EA in NEORL follow the paradigm in Algorithm 1. A random population is generated, evaluated by a fitness function, best individuals are selected for further evolution, and the population is updated using natural operations (crossover, mutation, hunting strategies, food search, etc.) for the next generation. The main differences between EA are the types of natural operations and how the population individuals are communicating. For example, GA uses mutation and crossover, PSO uses cognitive and social speed to communicate, while GWO uses prey search, encircle, and hunting methods.

Algorithm 1 Pseudocode for evolutionary algorithms (Minimization)

```

1: •Set algorithm hyperparameters
2: •Define the fitness function and input space
3: •Initialize the population randomly with size  $pop\_size$ , i.e.  $\{\vec{x}_1^0, \vec{x}_2^0, \dots, \vec{x}_{pop\_size}^0\}$ 
4: •Initialize  $y_{best} = \infty$ 
5: for Generation  $k = 1$  to  $N_{gen}$  do
6:   for Individual  $j = 1$  to  $pop\_size$  do
7:     •Encoding-decoding tools are applied to obtain the individual in real space ( $\vec{x}_j^0 \rightarrow \vec{x}_j$ )
8:     •Individual  $\vec{x}_j$  is evaluated by the fitness function, and fitness  $y_j$  is returned
9:     if  $y_j < y_{best}$  then
10:      •Set  $y_{best} = y_j$ 
11:      •Set  $\vec{x}_{best} = \vec{x}_j$ 
12:   •(Optional step) Select the top  $m$  individuals to survive to the next generation, i.e.  $m < pop\_size$ 
13:   •Update the population position using evolutionary operations to minimize fitness in the next generation
14: •Return  $\vec{x}_{best}$  and  $y_{best}$ 

```

We will highlight the Harris Hawks optimization (HHO) [21] as one of the most recent EA. HHO employs different approaches to update the Hawks positions, which are chasing a prey (global optima) to hunt. After evaluating the first random generation, $\vec{x}^{rabbitt}$ can be determined, which is the position of the closest hawk to the prey. In every subsequent generation, the following processes are applied for every hawk in the population. The energy of the prey is updated every generation using:

$$E = 2E_0(1 - k/N_{gen}), \quad (2)$$

where $E_0 = 2rand(0, 1) - 1$ is the baseline energy, k is the current generation, and N_{gen} is the total number of generations. Now if the absolute value of rabbit energy is more than 1, $|E| \geq 1$, the hawks activate the exploration phase expressed by:

$$\vec{x}_{k+1} = \begin{cases} \vec{x}_k^{rand} - r_1|\vec{x}_k^{rand} - 2r_2\vec{x}_k| & q \geq 0.5 \\ (\vec{x}_k^{rabbitt} - \vec{x}_k^m) - r_3(\vec{x}_{min} + r_4(\vec{x}_{max} - \vec{x}_{min})) & q < 0.5 \end{cases} \quad (3)$$

where \vec{x}_{k+1} is the updated position of the hawk in the next generation, $\vec{x}_k^{rabbitt}$ is the position of rabbit, \vec{x}_k is the current position of the hawk, and r_1, r_2, r_3, r_4, q are uniform random numbers between $[0, 1]$, which are regenerated in each new generation. \vec{x}_{min} and \vec{x}_{max} are the upper and lower bounds of the variables, \vec{x}_k^{rand} is a randomly selected hawk from the current population, and \vec{x}_k^m is the average position of the current population of hawks. As the reader can notice, significant amounts of randomness can be seen in Eq.(3), which are supposed to improve the exploration of the hawks in finding a prey. Now if $|E| < 1$, the hawks activate their exploitation phase, which involves one of four strategies. If $rand(0, 1) \geq 0.5$ and $|E| \geq 0.5$, hawks perform soft besiege of the prey by

$$\vec{x}_{k+1} = (\vec{x}_k^{rabbitt} - \vec{x}_k) - E|J\vec{x}_k^{rabbitt} - \vec{x}_k|, \quad (4)$$

where $J = 2(1 - rand(0, 1))$ represents the random jump strength of the rabbit, which is assumed to be a random jump. Otherwise, if $rand(0, 1) \geq 0.5$ and $|E| < 0.5$, hard besiege is applied as follows:

$$\vec{x}_{k+1} = \vec{x}_k^{rabbitt} - E|\vec{x}_k^{rabbitt} - \vec{x}_k|. \quad (5)$$

For brevity, the authors have added two more exploitation strategies where soft and hard besieges are conducted with progressive rapid dives toward the prey. Soft besiege with rapid dive occurs when $\{rand(0, 1) < 0.5 \text{ and } |E| \geq 0.5\}$, while hard besiege with rapid dive occurs when $\{rand(0, 1) < 0.5 \text{ and } |E| < 0.5\}$. The reader can refer to the original paper for more details about these exploitation strategies [21]. Overall, after sufficient number of generations, continuous update of the hawk positions will lead to a solution close to the global optima or the prey.

All EA in NEORL are completely or partially parallelized, where the population fitness is evaluated in parallel before the next position update. In particular, lines 6-11 of Algorithm 1 can be executed in parallel, as these steps, especially line 8, are usually the most expensive parts of EA. All EA supported in NEORL are listed in Table 1, including their supported input space.

2.2 Neural Networks Algorithms

Reinforcement learning (RL) algorithms are the main neural-based algorithms in NEORL due to their natural fit to optimization as described before in section 1. Indeed, all RL algorithms in NEORL belong to the subcategory of deep RL, as deep neural networks are trained based on RL reward signal. However, for simplicity, we will use the RL acronym in this work. The following terms in EA (individual, population size, fitness, generation, evolutionary operator) are analogous to the following terms in RL (action, episode length, reward, episode, agent update). The RL paradigm flow is shown in Figure 1 and described in Algorithm 2. The flow of RL and EA is quite similar with a major difference that the natural operators are replaced by a neural network model, which is trained continuously based upon the data collected from the fitness function. For optimization purposes, the action space (a_t) and state space (s_t) in Figure 1 are identical (see also line 10 in Algorithm 2). Notice that for consistency with EA, in Algorithm 2, we refer to the action a with symbol \vec{x} to represent the EA input individual. RL algorithms are usually classified into value-based, policy gradient, and actor-critic, with the later category being the state-of-the-art.

Algorithm 2 Pseudocode for reinforcement learning algorithms (Maximization)

- 1: •Set algorithm hyperparameters
 - 2: •Initialize the environment (i.e. fitness function and input space)
 - 3: •Initialize the neural network parameters (θ)
 - 4: •Initialize $y_{best} = -\infty$
 - 5: **for** Generation $k = 1$ to N_{gen} **do**
 - 6: **for** Agent $j = 1$ to pop_size **do**
 - 7: •Neural network proposes a base action (\vec{x}_j^0)
 - 8: •Encoding-decoding tools are applied to obtain the action in real space ($\vec{x}_j^0 \rightarrow \vec{x}_j$)
 - 9: •Action \vec{x}_j is evaluated by the environment, and fitness y_j is returned as reward
 - 10: •State is set to current action, $\vec{s}_j \leftarrow \vec{x}_j$
 - 11: **if** $y_j > y_{best}$ **then**
 - 12: •Set $y_{best} = y_j$
 - 13: •Set $\vec{x}_{best} = \vec{x}_j$
 - 14: •Update neural network parameters (θ) to maximize fitness in the next generation
 - 15: •Return \vec{x}_{best} and y_{best}
-

Q-learning or Quality-learning is the core of most value-based RL algorithms. In simple Q-learning, the Q value is updated recursively, as derived from the Bellman equation

$$Q^{new}(s_t, a_t) \leftarrow (1 - \alpha) \overbrace{Q(s_t, a_t)}^{\text{old value}} + \underbrace{\alpha}_{\text{learning rate}} \left[\underbrace{r_t}_{\text{reward}} + \underbrace{\gamma}_{\text{discount factor}} \cdot \underbrace{\max_a Q(s_{t+1}, a)}_{\text{optimum future value}} \right], \quad (6)$$

where s_t , a_t , and s_{t+1} are the current state, current action, and next state, respectively. Q-learning requires saving all state-action pairs in a Q-table, which can be extremely large and expensive for complex problems. Alternatively, neural networks are used to predict Q-value for each possible action, and then Q-learning can decide which action to take based on the predicted Q-values. Training deep neural networks to approximate the Q function is known as deep Q learning (DQN) [30], which resolves all computational hurdles facing Q-learning. DQN is part of NEORL. Unfortunately, DQN is restricted to discrete spaces.

This limitation inspires the development of the policy gradient family. PG aims to train a policy that directly maps states to appropriate actions without an explicit Q function in the middle, by optimizing the following loss function

$$L^{PG}(\theta) = E_t[\log \pi_\theta(a_t|s_t)A_t], \quad (7)$$

where E_t is the expectation over a batch of state-action pairs, π is the policy to be optimized which has weights θ . The policy π predicts action a given state s at time step t . The term A_t is called the advantage estimate, which expresses the discounted reward $A_t = \sum_{k=0}^{\infty} \gamma^k r_{t+k}$, where γ is the discount factor [54]. Most policy gradient algorithms like REINFORCE update the policy parameters through Monte Carlo or random sampling, which introduces high variability in the log of the policy distribution and the reward values (and so A_t), leading to unstable learning. This limitation inspired the ‘‘actor-critic’’ family with a goal to reduce variance and increase stability through subtracting the discounted

reward by a baseline term V as follows

$$A_t = \underbrace{\sum_{k=0}^{\infty} \gamma^k r_{t+k}}_{\text{Discounted Reward}} - \underbrace{V(s_t)}_{\text{Baseline (or VF) Estimate of Discounted Reward}}, \quad (8)$$

where r is the reward value, γ is the discount factor, and V is the baseline or value function (VF) estimate of the discounted reward. The VF baseline makes the cumulative reward smaller, which makes smaller gradients, and more stable updates. The actor-critic algorithms involve two major phases:

- The ‘‘Critic’’ phase, which estimates the VF, which could be a Q value.
- The ‘‘Actor’’ phase, which updates the policy parameters in the direction suggested by the Critic.

Both the critic and the actor functions are parameterized with neural networks, which are updated continuously to maximize the reward return. The NEORL supported algorithms from actor-critic are Advantage Actor Critic (A2C), Actor-Critic with Experience Replay (ACER), Proximal Policy Optimization (PPO), and Actor Critic using Kronecker-Factored Trust Region (ACKTR). See Table 1 for the full list of the neural-based algorithms within NEORL and their supported spaces. We leveraged our RL optimization classes following the RL implementation provided by OpenAI baselines [36] and stable-baselines [37].

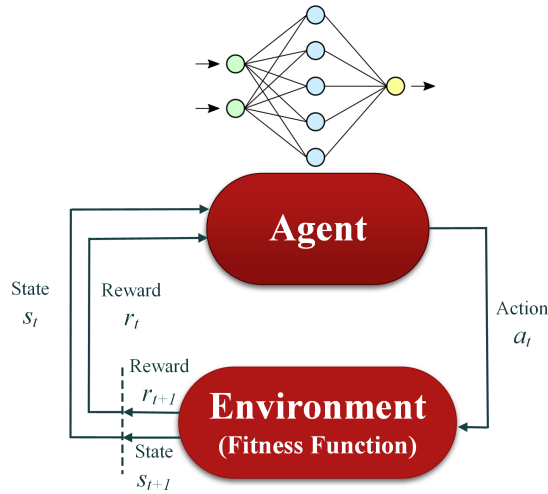


Figure 1: Reinforcement learning flow for optimization

2.3 Neuroevolution Algorithms

The category of neuroevolution refers to a class of hybrid algorithms in our framework that utilizes both neural network and evolutionary computation concepts to obtain the best of both worlds. NEORL supports NEAT [38] for optimization with two different architectures: feedforward neural networks (called FNEAT) and recurrent neural networks (called RNEAT). In both algorithms, GA is used to leverage neural network topology to maximize a fitness function of interest.

We also provide an implementation for RL-informed EA, a concept developed by the authors [44]. Using RL as a seeding methodology can be effective to improve the exploration rate of EA in constrained optimization problems. RL algorithms can run as a standalone to generate certain individuals matching part of the problem constraints. Then these RL quality individuals are periodically mixed with EA population to lead to a better search and less local optima entrapment. Currently, in NEORL, the neuroevolution PPO-ES is implemented, where PPO is used to guide genetic algorithms or evolution strategies as illustrated by this large-scale nuclear assembly combinatorial optimization [55]. In addition, we provide an implementation of ACKTR-DE as another neuroevolution alternative that can be promising for continuous optimization. Both of these neuroevolution algorithms feature parallel search.

NEORL provides support for a high-performance hybrid algorithm called PESA (Prioritized replay Evolutionary and Swarm Algorithm), which combines the concept of experience replay with hybrid evolutionary algorithms [56, 57], another concept developed by the authors. Two modes of experience replay are introduced into PESA: prioritized replay

to enhance exploration and greedy replay to improve algorithm exploitation. The replay memory stores all individuals in a shared memory across the hybrid algorithms, and replays them with different rates based on their fitness value, such that exploration and exploitation can be balanced during search. Two variants of PESA are currently available in NEORL. Classical PESA, which combines GA, PSO, and SA, and it proved to be effective in discrete optimization. Modern PESA2, which hybridizes GWO, DE, and WOA, proved to be effective in continuous optimization. PESA and PESA2 are candidates to solve expensive problems when computing power is available, as both PESA variants are fully parallelized with parallel efficiency $> 85\%$ when tested on 200 processors.

For expensive optimization with limited computing power, NEORL offers hybrid neuroevolution algorithms, where neural networks act as surrogate models to assist EA search. Currently, we provide an implementation of the recent offline data-driven evolutionary optimization concept [58], where only small number of fitness evaluations are needed to build a surrogate model, such that the surrogate can replace the original fitness function in EA optimization. The original implementation involves using surrogate models of radial basis function networks to assist GA. The authors extend this methodology to more modern algorithms, where we use deep feedforward neural networks as surrogate models through TensorFlow to assist HHO described in section 2.1, where all discrete, continuous, and mixed-discrete spaces are handled. In addition, compared to [58], the neuroevolution Harris hawks optimizer offers parallel training of the surrogate models as well as parallel evaluation of the initial hawks used to construct the surrogate models. These surrogate-based neuroevolution algorithms are useful for large-scale optimization problems with limited computing power. Lastly, Table 1 shows a summary of all hybrid neuroevolution algorithms in NEORL and their supported spaces.

2.4 Multiobjective Optimization and Constrained Handling

Without loss of generality, multiobjective optimization can be formulated as follows:

$$\begin{aligned} \min_{\vec{x}} F(\vec{x}) &= (f_1(\vec{x}), f_2(\vec{x}), \dots, f_k(\vec{x})) \\ \text{subject to,} \\ g_i(\vec{x}) &\geq 0, \quad i = 1, 2, \dots, m, \\ h_j(\vec{x}) &= 0, \quad j = 1, 2, \dots, p, \\ k &\geq 2, \end{aligned} \tag{9}$$

where k is the number of objective functions. The set of solutions \vec{x} that satisfies all constraints defines the feasible region Ω , i.e. $\vec{x} \in \Omega$.

Solving multiobjective optimization can be done either through solving the problem directly by trying to optimize each objective through using posteriori methods, or through using priori methods, which what we currently support in NEORL. Priors methods involve the users by specifying their preferences beforehand to formulate a single-objective optimization problem, such that optimal solutions to the single-objective problem are feasible solutions to the multi-objective problem. Linear scalarization, ϵ -constrained, achievement scalarizing function, and Sen’s Multi-Objective Programming are among the common priori methods [59].

The usage of priori methods is advantageous for NEORL, since the formulation of the fitness function will be consistent across EA, neural networks, and neuroevolution. RL algorithms are expected reward (fitness) as a scalar value. Adding special algorithms to NEORL for multiobjective optimization such as non dominated sorting genetic algorithm (NSGA-II) is left for future releases. Currently, to preserve a generic implementation, the user can use variety of priori methods to convert multiobjective to single objective problem. Indeed, NEORL demonstrated successful results with complex multiobjective optimization problems, which are illustrated here [34, 55, 44], where ϵ -constrained and linear scalarization in conjunction with different neural, evolutionary, and neuroevolution algorithms have been effective in solving the multiobjective optimization.

For constraint handling, we give the user the freedom to handle the constraints internally within the fitness function, before returning the fitness value to the optimizer. This flexibility gives the user a chance to explore different constraint handling methods on the same problem such as applying hard penalty, self-adaptive penalty, or ϵ -constrained [60].

3 NEORL Structure

In this section, we briefly describe the main steps to do to setup and solve an optimization problem via NEORL.

3.1 Fitness/objective Function

The fitness function is problem or user-dependent and it is the only NEORL step that depends significantly on the user and application of interest. The fitness function can be as simple as a mathematical function or as complex as a fitness function that has to deal with computer code execution, input handling, and output post-processing. In both cases, the format of the fitness function is similar, it takes input as the vector of input parameters to optimize (\vec{x}) and returns output as the scalar fitness value corresponding to this \vec{x} . See Python Listing 1 for a simple fitness function of the multi-dimensional sphere that has the form

$$f(\vec{x}) = \sum_{i=1}^d x_i^2, \quad (10)$$

where d is the number of dimensions (degrees of freedom) of the Sphere, and it is equal to the size of the input vector \vec{x} . For complex fitness functions, the user needs to code more lines to reach the final scalar “ y ” value returned by the function.

```
1 def Sphere(x):
2     y=sum(xi**2 for xi in x)
3     return y
```

Listing 1: Example of a NEORL fitness function definition

An additional example on defining advanced fitness function for constrained optimization can be found in Python Listing 2 using self-adaptive penalty proposed by [61]. The single-objective constrained problem is for the three-bar truss design, which is a popular constrained optimization problem described here [19]. The problem has three constraints and two input variables to optimize, which are related to the bars’ cross-sectional area. Similarly, for multiobjective optimization, the user can change line 24 in Listing 2 to a weighted sum of all objectives if linear scalarization is used to convert multiobjective optimization to single objective.

```
1 from math import sqrt
2 def TBTD(x):
3     """
4     Three-Bar Truss Design
5     See Supplementary Materials Section 2.1 for the Mathematical Description
6     """
7     x1 = x[0] #A1=A3 (cross-sectional area)
8     x2 = x[1] #A2 (second cross-sectional area)
9     y = (2*sqrt(2)*x1 + x2) * 100 #objective value (volume of loaded truss structure)
10
11 #Constraints
12 g1 = (sqrt(2)*x1+x2)/(sqrt(2)*x1**2 + 2*x1*x2) * 2 - 2 #g1 <= 0 is required
13 g2 = x2/(sqrt(2)*x1**2 + 2*x1*x2) * 2 - 2 #g2 <= 0 is required
14 g3 = 1/(x1 + sqrt(2)*x2) * 2 - 2 #g3 <= 0 is required
15 g = [g1,g2,g3]
16
17 #penalty coefficients
18 w1=100 # coefficient for self-adaptive penalty (Coello, 2000)
19 w2=100 # coefficient for self-adaptive penalty (Coello, 2000)
20
21 #final fitness value
22 phi=sum(max(item,0) for item in g) #sum of all constraint values
23 viol=sum(float(num)>0 for num in g) #sum of the number of violated constraints
24 fitness =y + w1*phi + w2*viol #penalized fitness value
25
26 return fitness
```

Listing 2: Example of a NEORL fitness function for constrained optimization

3.2 Input Search Space

NEORL supports three types of input spaces: discrete variable (labelled by `int`), continuous variable (labelled by `float`), and categorical variable (labelled by `grid`). A mixed space of the three types is also possible to define. A discrete variable is expected to take integer values, where the label `int` is followed by the lower and upper bounds

allowed. The continuous variable takes real values, where the label `float` is followed by the lower and upper bounds allowed. The categorical variable takes fixed values defined by a grid, where the label `grid` is followed by the list of values as a tuple (i.e. enclosed in a parenthesis), e.g. (value 1, value 2, ...). The values in the grid can be integers, real, and/or of string type. NEORL expects the full parameter space to be defined in Python dictionary (`dict`) format. See Listing 3 which demonstrates two examples of how to define an input space \vec{x} with NEORL. In addition, all possibilities of input spaces are defined in Table 2 with a demonstration example. The reader can check the space types that each NEORL algorithm supports in Table 1.

```

1 #A real-valued input space of size 5
2 d=5
3 Space1={}
4 for i in range(1,d+1):
5     Space1['x'+str(i)]=['float', -100, 100] #5 continuous variables between -100/100
6 #A mixed input space of size 4
7 Space2 = {}
8 Space2['n_layers'] = ['int', 1, 6] #number of layers in a network as integer
9 Space2['n_nodes'] = ['int', 50, 150] #number of nodes in each layer as integer
10 Space2['activation'] = ['grid', ('linear', 'rbf', 'sigmoid')] # activation type as categorical
11 Space2['learning_rate'] = ['float', 1e-4, 1e-3] #learning rate as continuous variable

```

Listing 3: Example of a NEORL search space definition

Table 2: Input space types supported by NEORL

Space Type	Example
Combinatorial/Discrete	space['x1'] = ['int', 1, 6] space['x2'] = ['int', 50, 150] space['x3'] = ['int', -10, 10]
Categorical	space['x1'] = ['grid', (1, 2, 3, 4, 5, 6)] space['x2'] = ['grid', ('linear', 'rbf', 'sigmoid')] space['x3'] = ['grid', (1.5, 2.5, 3.5, 4.5)]
Continuous	space['x1'] = ['float', 1, 6] space['x2'] = ['float', 50, 150] space['x3'] = ['float', -10, 10]
Mixed Discrete/Categorical	space['x1'] = ['int', 1, 6] space['x2'] = ['grid', ('linear', 'rbf', 'sigmoid')] space['x3'] = ['grid', (1, 2.5, 5, 10)]
Mixed Discrete/Continuous	space['x1'] = ['int', 1, 6] space['x2'] = ['float', 50, 150] space['x3'] = ['float', -10, 10]
Mixed Categorical/Continuous	space['x1'] = ['float', -100, 100] space['x2'] = ['grid', ('linear', 'rbf', 'sigmoid')] space['x3'] = ['grid', (1, 2.5, 5, 10)]
Mixed Discrete/Continuous/Categorical	space['x1'] = ['int', 1, 6] space['x2'] = ['grid', ('linear', 'rbf', 'sigmoid')] space['x3'] = ['float', -10, 10]

3.3 Algorithms

Every algorithm class in NEORL is expecting multiple arguments to establish an algorithm instance, which can be grouped into: (1) problem-based, (2) algorithm hyperparameters, and (3) miscellaneous. The problem-based arguments are the `mode` of the problem (minimization or maximization), the `bounds` which is the parameter space defined in section 3.2, and the fitness function (`fit`) defined in section 3.1. Algorithm hyperparameters are specific to each algorithm, which usually need to be tuned by the user for optimal performance. Miscellaneous arguments may include the random `seed` for reproducibility and `ncores` for multiprocessing (see section 3.4). After defining an algorithm

instance, the user can start the optimization process by a special method called `.evolute` for evolutionary algorithms and `.learn` for neural and RL algorithms.

For EA, these methods expect number of generations/iterations to run the optimizer for (e.g. `ngen`), an initial guess `x0` if applicable (if `x0=None` the optimizer starts with a random guess), and `verbose` to print the progress. See Listing 4, which shows two examples of setting and evolving a grey wolf and a simulated annealing optimizer. The listing shows that number of wolves in the group (`nwolves`) and size of the annealing chain before update (`chain_size`) are a few examples of the hyperparameters of these algorithms. At the end of evolution, the optimizer returns three variables: `xbest`, `ybest`, and `log`, which are respectively: (1) the best value of the input vector \vec{x} , the best value of the fitness y , and a logger in dictionary form containing major statistics as found by the optimizer.

```

1 from neorl import GWO, SA #import the classes
2 #Grey Wolf Optimization (setup and evolution)
3 gwo=GWO(mode='min', fit=Sphere, bounds=Space1, nwolves=5, ncores=1, seed=1)
4 xbest, ybest, log=gwo.evolute(ngen=100, x0=None, verbose=True)
5
6 #Simulated Annealing (setup and evolution)
7 sa=SA(mode='min', fit=Sphere, bounds=Space1, chain_size=30, chi=0.2, ncores=1, seed=1)
8 xbest, ybest, log=sa.evolute(ngen=100, x0=None, verbose=True)

```

Listing 4: Example of NEORL evolutionary algorithm setup

For neural algorithms, these methods expect definition of special classes to be compatible with the RL paradigm (action, state, reward, etc.). Listing 5 shows how to set and evolve a PPO optimizer. First, a RL environment is constructed by passing some problem-based arguments such as the fitness function (`fit`), the bounds of the input space (`bounds`), problem mode (`mode`), number of processors (`ncores`), and the length of the episode in time steps (`episode_length`). Afterwards, the user defines a logger using the method `RLLogger` which records samples during training with frequency `check_freq`. The PPO object can then be constructed by defining the policy type such as feedforward policy (`MlpPolicy`), passing the created environment instance (`env`), and a set of PPO hyperparameters (e.g. `n_steps`, `ent_coef`). The learning process can be started using the `.learn` method. The user should notice here that neural algorithms `learn` function expects a total of fitness evaluations in time steps (`total_timesteps`). The user can calculate the number of generations as in EA by simply taking the ratio of `total_timesteps` over `episode_length`. Finally, the user can access the best solutions from the callback function via the variables: `cb.xbest` and `cb.rbest`.

```

1 from neorl import PPO2, MlpPolicy, RLLogger, CreateEnvironment
2
3 #For neural algorithms, create an environment that includes the fitness, space type, and problem mode (min/max)
4 env=CreateEnvironment(method='ppo', fit=Sphere, bounds=Space1, mode='min', ncores=1, episode_length=50)
5 cb=RLLogger(check_freq=1, save_model=True) #create a callback function to log data every step
6 #MlpPolicy is a feedforward multilayer perceptron neural network policy
7 ppo = PPO2(MlpPolicy, env=env, n_steps=12, ent_coef=0.01, seed=1) #create a PPO object based on the defined env
8 #number of generations = total_timesteps / episode_length
9 ppo.learn( total_timesteps =2000, callback=cb) #optimize the environment fitness
10 #access optimal results
11 print('The best value of x found:', cb.xbest)
12 print('The best value of fitness found:', cb.rbest)

```

Listing 5: Example of NEORL neural algorithm setup

3.4 Parallel Computing

Parallel optimization is crucial to accelerate the process if the fitness function is very expensive to evaluate (e.g. requires running a computer code). Fortunately, invoking parallel optimization via NEORL is very straightforward via the argument `ncores`, where the user specifies number of processors to use, see Listing 4-5. Currently, majority of NEORL algorithms support parallel/multiprocessing optimization (see Table 1).

Figure 2 compares parallel optimization performance of four different algorithms from the three different categories in optimizing the sphere function. The sphere function is delayed by 1s to reflect expensive optimization and to avoid conflict with parallel overhead costs. All algorithms have been executed for 20 generations and 32 individuals per

generation using 1, 8, 16, and 32 processors. First we can notice a large decrease in computational time when increasing the number of processors for all four algorithms. Second, we can notice that HHO is significantly slower than other algorithms, even compared to its closest EA fellow, GWO. The algorithm steps of GWO can be completely parallelized due to the nature of the algorithm. However, HHO algorithm has some serial steps, in particular, when executing soft and hard besieges, which require dependency between the population individuals. This makes HHO multiprocessing slower than GWO. Third, we can see that PESA is slower than PPO and GWO when using single processor, while its superior performance is clearly observed after activating its two-levels of parallelism. Overall, in Figure 2, moving from 1 processor to 32, the speedup factor of HHO is only 3, GWO is 30, PPO is also 30, and PESA is 46.

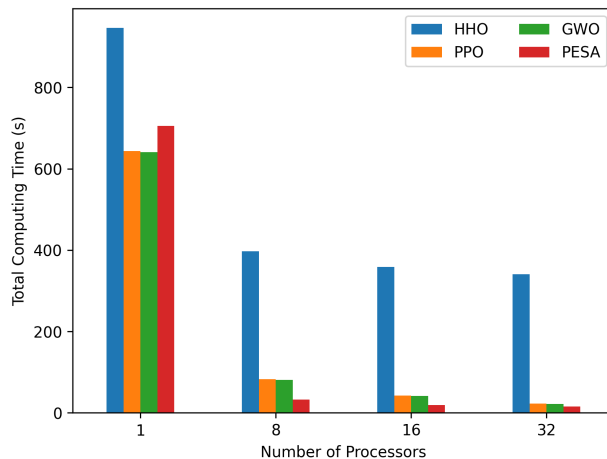


Figure 2: Comparison of multiprocessing performance of different NEORL algorithms

3.5 Restart Capabilities

NEORL provides restart capabilities for the user to restart the search from a recent checkpoint. This feature is useful for long optimization runs, when the search could terminate due to technical issues or power outage. For the RL neural optimizers, the neural network model can be saved periodically using the flag `save_model` in the `RLLogger`, see line 5 of Listing 5. Similarly, for the evolutionary or neuroevolution optimizers, the user can use the argument `x0` (see line 4 or line 8 of Listing 4), to specify the initial population. The user can recover a population using the best individuals of the previous generations, and use that population to continue the search.

3.6 Hyperparameter Tuning

In certain cases when the problem is high-dimensional and the fitness function is very expensive and complex, the performance of the algorithms may become sensitive to their hyperparameters (e.g. `nwolves`, `chi`, `chain_size`, `n_steps`). To keep the user isolated from the tedious burden of manual and trial-and-error tuning, NEORL provides four systematic and automatic methods to assess the optimizer performance under different combination of hyperparameters for a certain problem/fitness setup. The top hyperparameter sets are reported by these methods for the user to use for further analysis. The tuning methods are: exhaustive grid search, random search, Bayesian search, and evolutionary search. In addition, most of these methods support parallel search to significantly accelerate the tuning process. We refer the user to this link³, which contains a Python example of how to use NEORL grid search, and other methods can be accessed from the same webpage.

We compare the hyperparameter search algorithms in tuning ES/GA to minimize a 20-dimension sphere function of Eq.(10). We target three hyperparameters of ES: `cxpb`, `mutpb`, and `alpha`, which are respectively the crossover probability, mutation probability, and probability of blending during crossover (i.e. all hyperparameters have a range of 0 to 1). All four methods have been executed to evaluate 100 combinations of the previous hyperparameters, and the minimum fitness of every 10 combinations is plotted in Figure 3 for consistency across methods. All methods seem to perform in a comparable manner given the converged fitness is close between the four methods. Bayesian and evolutionary methods seem to show quicker convergence than grid and random searches due to their systematic

³Grid Search: <https://neorl.readthedocs.io/en/latest/tune/grid.html>

search behaviour. Bayesian search found the best hyperparameter set as follows: `cspb = 0.8`, `mutpb = 0.2`, and `alpha = 0.424`.

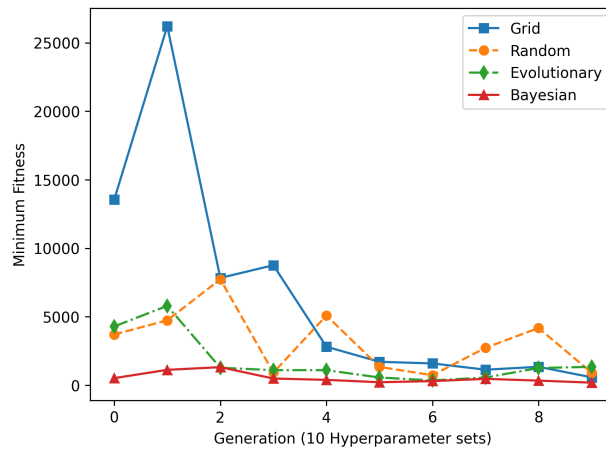


Figure 3: Comparison of the hyperparameter tuning algorithms in NEORL

Lastly, we end this section by Listing 6, which shows how to setup a full optimization problem in NEORL with few lines. The problem in Listing 6 shows how to optimize the 5-d Sphere function of Eq.(10) with the grey wolf optimizer (GWO). To further validate NEORL capabilities, the framework is benchmarked against a variety of mathematical functions, which are not reported here for brevity and kept for the full paper.

```

1 from neorl import GWO
2 #Setup the fitness function
3 def Sphere(x) :
4     y=sum(xi**2 for xi in x)
5     return y
6 #Setup the parameter space
7 d=5
8 Space={}
9 for i in range (1, d+1):
10     Space['x'+str(i)]=['float', -100, 100]
11 #Setup and evolve the optimizer
12 gwo=GWO(mode='min', fit=Sphere, bounds=Space, nwoles=5, ncores=1, seed=1)
13 xbest, ybest, log=gwo.evolute(nngen=100, verbose=1)
14 print('Best input: ', xbest)
15 print('Best fitness: ', ybest)
16 #which prints these after running:
17 #Best input: [0.00015237, -0.0002251, 0.00023039, -0.00016578, 0.00019899]
18 #Best fitness : 1.9404338787767446e-07

```

Listing 6: NEORL full example of optimizing the 5-d Sphere

3.7 Comparison with Other Frameworks

Table 3 compares NEORL to the popular Python optimization frameworks based upon different features that each user prioritizes. The comprehensive nature of NEORL is clearly displayed. For gradient-based algorithms, they are not explicitly implemented in NEORL due to the fact that these algorithms are well-supported in other frameworks such as PyOpt [52] and nlopt [51]. NEORL provides access to more algorithms, diverse algorithm types, hyperparameter tuning, parallel computing, detailed documentation, and real-world engineering examples. Here we can highlight that “PyOpt” [52] is recommended for gradient-based algorithms, even though the framework is not continuously maintained or updated by the authors. Also, “PyOpt” is only restricted to the legacy Python 2, which is superseded by the modern Python 3. “nlopt” [51] provides robust gradient-based and evolutionary algorithms, however, without parallel support or detailed documentation of the Python plugin. “Evolopy” [26] provides a good Python implementation of modern evolutionary algorithms (e.g. GWO, WOA, SSA), while the framework seems to lack detailed documentation, parallel computing, and tests on large-scale problems. Lastly, “DEAP” [25] is undoubtedly the most popular evolutionary

optimization framework when it comes to genetic algorithms and evolution strategies, with a detailed documentation and real-world examples. Nevertheless, the lack of support of modern EA, neural algorithms, and hybrid neuroevolution can be considered as an advantage for NEORL over DEAP.

Table 3: Comparison of NEORL with other popular Python optimization frameworks

Feature	NEORL	PyOpt [52]	EvoPy [26]	nlopt [51]	DEAP [25]
Number of Algorithms	28	20	14	23	5
Classical Evolutionary Computation	✓	✓	✓	✓	✓
Modern Evolutionary Computation	✓	×	✓	×	×
Neural Networks	✓	×	×	×	×
Gradient-based Algorithms	✓*	✓	×	✓	×
Hybrid Algorithms	✓	×	×	×	×
Hyperparameter Tuning	✓	×	×	×	×
Parallel Computing	✓	✓	×	×	✓
Detailed Documentation	✓	✓	×	×**	✓
Real-world Examples	✓	✓	×	×**	✓

* Gradient-based algorithms in NEORL are embedded as optimizers of the neural networks

** `nlopt` is implemented in different programming languages, the Python plugin is not thoroughly documented/benchmarked.

4 Applications

In this section, we apply NEORL to two different carbon-free energy applications on fuel cell power production (continuous optimization) and nuclear reactor control (mixed discrete-continuous optimization) to demonstrate NEORL potential to help combating climate change. Links for additional NEORL applications are listed by the end of this section.

4.1 Fuel Cell Design Optimization

A solid oxide fuel cell (SOFC) converts chemical energy into electricity via the oxidation of a fuel, typically hydrogen [62, 63]. The topic of fuel cell design optimization is continuously researched to improve the power output and efficiency using variety of optimization, uncertainty analysis, and machine learning methods [64, 65, 66, 67]. Here we seek a similar objective to optimize various operating parameters of a SOFC with the goal of maximizing both the power output, P , and the efficiency, η , consolidated into a single objective function given by

$$\max_{\vec{x}} f(\vec{x}) = 0.5 \times P + 0.5 \times \eta \times 100. \quad (11)$$

The voltage in the fuel cell is calculated as

$$V_{cell} = E - V_{act} - V_{ohm} - V_{conc}, \quad (12)$$

where E is the maximum voltage, V_{act} is the activation overpotential due to electrode kinetics, V_{ohm} is the ohmic overpotential associated with electrical resistance, and V_{conc} is the concentration overpotential caused by resistance to the movement of reactants and products [68].

The maximum voltage is expressed as

$$E = \frac{-\Delta g}{n_e F} + \frac{RT}{n_e F} \ln \left(\frac{p_{H_2} p_{O_2}^{0.5}}{p_{H_2O}} \right), \quad (13)$$

where $\Delta g = -282150 + 86.735T$ is the Gibbs free energy change, n_e is the number of electrons per reaction, F is Faraday's constant, R is the universal gas constant, T is the operating temperature of SOFC, and p_{H_2} , p_{O_2} , and p_{H_2O} are the partial pressure of hydrogen (H_2), oxygen (O_2), and water (H_2O), respectively [68].

The total activation overpotential is the sum of both the anode and cathode parts, $V_{act,a}$ and $V_{act,c}$. The equation for $V_{act,k}$ for $k = a, c$ is [62, 63, 69]

$$\begin{aligned} V_{act,k} &= \frac{RT}{F} \sinh^{-1} \left(\frac{j}{2j_{0,k}} \right) \\ &= \frac{RT}{F} \ln \left[\frac{j}{2j_{0,k}} + \sqrt{\left(\frac{j}{2j_{0,k}} \right)^2 + 1} \right] \quad (k = a, c), \end{aligned} \quad (14)$$

where j is the operating current density and $j_{0,k}$ is the exchange current density at either the anode or the cathode. The exchange current densities at the anode and cathode are given respectively as [62, 63, 69]

$$j_{0,a} = \gamma_a \frac{72X[D_p - (D_p + D_s)\epsilon]\epsilon}{D_s^2 D_p^2 (1 - \sqrt{1 - X^2})} \times \left(\frac{p_{H_2}}{p}\right) \left(\frac{p_{H_2O}}{p}\right) \exp\left(-\frac{E_{act,a}}{RT}\right), \quad (15)$$

and

$$j_{0,c} = \gamma_c \frac{72X[D_p - (D_p + D_s)\epsilon]\epsilon}{D_s^2 D_p^2 (1 - \sqrt{1 - X^2})} \times \left(\frac{p_{O_2}}{p}\right)^{0.25} \exp\left(-\frac{E_{act,c}}{RT}\right), \quad (16)$$

where γ_a and γ_c are the coefficients of exchange current density at the anode and cathode, X is the ratio of grain contact neck length to the grain size, D_p and D_s are pore size and grain size, respectively, ϵ is the electrode porosity, p is the operating pressure, and $E_{act,a}$ and $E_{act,c}$ are the activation energy for the anode and cathode, respectively.

The ohmic overpotential is given by [62]

$$V_{ohm} = j \left(\frac{L_a}{\sigma_a} + \frac{L_c}{\sigma_c} + \frac{L_e}{\sigma_e} \right), \quad (17)$$

where L_a , L_c , and L_e are the thicknesses of the anode, cathode, and electrolyte, respectively and σ_a and σ_c are the electric conductivity of the anode and cathode, respectively. The ionic conductivity of the electrolyte, σ_e , is

$$\sigma_e = \exp(-1.03 \times 10^4/T). \quad (18)$$

Finally, the concentration overpotential can be expressed as the sum of the anode and cathode parts, $V_{conc,a}$ and $V_{conc,c}$. At the anode, the concentration overpotential is

$$V_{conc,a} = \frac{RT}{n_e F} \left[\ln \left(1 + \frac{j}{j_{lH_2O}} \right) - \ln \left(1 - \frac{j}{j_{lH_2}} \right) \right], \quad (19)$$

where $j_{lH_2O} = 2.27 \times 10^7 \text{ A m}^{-2}$ and $j_{lH_2} = 4 \times 10^5 \text{ A m}^{-2}$ [68].

At the cathode, the concentration overpotential is [62, 63, 69]

$$V_{conc,c} = \frac{RT}{4F} \ln \left[\frac{p_{O_2}}{\frac{p_c}{D} - \left(\frac{p_c}{D} - p_{O_2} \right) \exp \left(\frac{RTL_c j D}{4FD_{O_2}^{eff} p_c} \right)} \right], \quad (20)$$

where $p_c = p_{O_2} + p_{N_2}$ is the operating pressure on the cathode, $D_{O_2}^{eff}$ is the effective diffusion coefficient of the O_2 species, and D is the ratio of diffusion coefficients, $D = D_{O_2,Kn}^{eff} / (D_{O_2,Kn}^{eff} + D_{O_2-N_2}^{eff})$.

All of these equations are combined back into Eq.(12), so the power output and efficiency can be calculated respectively as

$$P = jAV_{cell} \quad (21)$$

and

$$\eta = \frac{P}{-\Delta \dot{H}} = -\frac{n_e F V_{cell}}{\Delta h}, \quad (22)$$

where $\Delta \dot{H} = (\Delta h/n_e F)jA$ is the total energy content of the SOFC fuel per unit time.

In total there are 20 uncertain parameters to be optimized with lower and upper bounds shown in Table 4. The bounds are derived from the distributions outlined by [68], where parameters with uniform distributions are optimized over their entire domain, while parameters with normal distributions are bounded within four standard deviations of the mean. In this analysis, the operating temperature T is held constant.

This problem is solved using differential evolution (DE), bat algorithm (BAT), grey wolf optimizer (GWO), moth-flame optimization (MFO), and modern PESA (PESA2) within NEORL. Each algorithm is executed for 300 generations with 50 individuals for a total of 15000 fitness evaluations. In addition, Bayesian search is applied to 3 algorithms: BAT, PESA2, and DE for 30 iterations to tune their hyperparameters with reduced number of generations per iteration. GWO and MFO are not tuned as they are considered hyperparameter-free, since we fixed the population size between the five algorithms. Figure 4 shows the convergence of the Bayesian hyperparameter tuner for DE, BAT, and PESA2. We can notice that the Bayesian search results indicate finding an optimal hyperparameter set within 15 iterations, which is very efficient. Also, the results show large sensitivity of PESA2 to its hyperparameters (which is expected for hybrid

Table 4: The upper and lower bounds of all 20 uncertain parameters in the fuel cell

Parameter	Bounds
Current density, j^* ($A m^{-2}$)	[12672, 13728]
Effective surface area, A (m^2)	$[1.55 \times 10^{-3}, 1.65 \times 10^{-3}]$
Partial pressure of O_2 , p_{O_2} (atm)	[0.168, 0.252]
Partial pressure of H_2O , p_{H_2O} (atm)	[0.04, 0.06]
Electrode porosity, ϵ	[0.3936, 0.5664]
Electrode tortuosity, ξ	[4.32, 6.48]
Average pore diameter, D_p (m)	$[2.8 \times 10^{-6}, 3.2 \times 10^{-6}]$
Average grain size, D_s (m)	$[1.4 \times 10^{-6}, 1.6 \times 10^{-6}]$
Average length of grain contact, X	[0.6, 0.8]
Anode thickness, L_a (m)	$[4.7 \times 10^{-4}, 5.3 \times 10^{-4}]$
Cathode thickness, L_c (m)	$[4.7 \times 10^{-5}, 5.3 \times 10^{-5}]$
Electrolyte thickness, L_e (m)	$[4.7 \times 10^{-5}, 5.3 \times 10^{-5}]$
Anode electric conductivity, σ_a ($\Omega^{-1} m$)	[48000, 112000]
Cathode electric conductivity, σ_c ($\Omega^{-1} m$)	[5040, 11760]
Diameters of the H_2 molecular collision, σ_{H_2} (°)	[2.159, 3.495]
Diameters of the H_2O molecular collision, σ_{H_2O} (°)	[2.009, 3.273]
Diameters of the O_2 molecular collision, σ_{O_2} (°)	[2.635, 4.299]
Diameters of the N_2 molecular collision, σ_{N_2} (°)	[2.886, 4.710]
Anode coefficient of the exchange current density, γ_a (A m)	$[1.39 \times 10^{-9}, 1.69 \times 10^{-9}]$
Cathode coefficient of the exchange current density, γ_c (A m)	$[5.27 \times 10^{-10}, 6.44 \times 10^{-10}]$

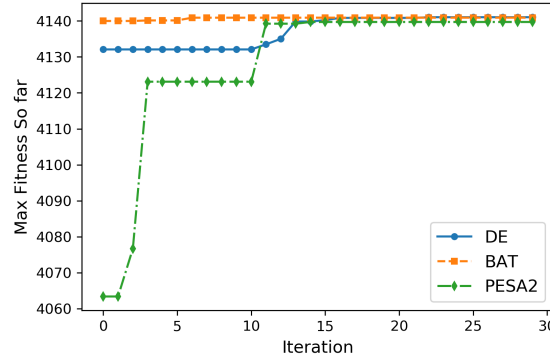


Figure 4: The convergence of the fuel cell fitness function using Bayesian hyperparameter tuning on DE, BAT, and PESA2 (GWO and MFO are hyperparameter-free).

algorithms), followed by DE. However, we can see that BAT has small sensitivity, as BAT fitness slightly improved during hyperparameter search.

The convergence of the fuel cell fitness function for the five algorithms under their optimal hyperparameters is shown in Figure 5 after running for 300 generations. Identical maximum solutions are found by DE, BAT, MFO, and PESA2 with a fitness value of 4141.4011, corresponding to $P = 8236.16 W$ and $\eta = 46.64\%$. Although most algorithms converge to similar solutions, PESA2 and MFO show faster convergence than other algorithms as in Figure 5. The best solution represents a significant improvement of 31% increase in power and a 26% increase in efficiency compared to the original design reported in the literature [68] using manual trial-and-error optimization based on expert knowledge. A comparison of our results to the literature is shown in Table 5. These significant improvements in power output and efficiency show NEORL potential to optimize fuel cell designs for carbon-free energy production.

Fuel cells have several benefits over conventional combustion-based technologies. Fuel cells as found in Table 5 can operate with efficiency close to 47%, while most combustion engines provide a thermal efficiency of 20%. The fuel cell efficiency can be even higher for other fuel cell designs, such as Alkaline fuel cells whose efficiency ranging from 60%-70%. In addition, fuel cells have zero carbon emissions compared to combustion engines. Hydrogen fuel cells like SOFC emit only water and feature no air pollutants that create smog and cause health problems.

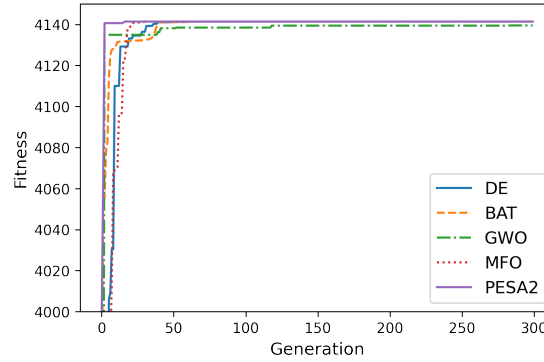


Figure 5: The convergence of the fuel cell fitness function using DE, BAT, GWO, MFO, and PESA2

Table 5: A comparison of the optimal fuel cell power and efficiency calculated with different algorithms

Method	Power (W m^{-2})	Efficiency
DE	8236.1574	46.64%
BAT	8236.1574	46.64%
GWO	8232.3813	46.62%
MFO	8236.1574	46.64%
PESA2	8236.1574	46.64%
Original SOFC [62, 68]	≈ 6300	$\approx 37.0\%$

4.2 Optimizing Neural Networks for Nuclear Reactor Control

The research on using machine and deep learning neural networks for nuclear reactor analysis is well-established. Examples of successful applications include using neural networks to predict nuclear power plant dynamic behaviour [70, 71], data-drive modeling of boiling heat transfer [72], nuclear multiphysics modeling [73], uncertainty quantification of multiphase flow [74], and similar others. The Massachusetts Institute of Technology (MIT) research reactor was constructed in 1956 and upgraded in 1974. The reactor is a light-water cooled reactor with 6 MW thermal power. The primary applications of the reactor are research applications such as irradiation experiments to test nuclear materials for large nuclear power plants. Top view of the MIT reactor is shown in Figure 6. The reactor core contains a total of 27 locations, where 5 locations are used for in-core experiments (A-1, A-3, B-3, B-6, B-9), and 22 locations are occupied by nuclear fuel elements. Each fuel element has a rhomboidal plate-type shape of highly enriched uranium oxide fuel in a dispersed aluminium matrix (see Figure 6). The reactor fuel positions are surrounded by six control blades (CB), located around the outer periphery of the core, which are strong neutron absorbers used for fission reaction control. Controlling the insertion depth of each CB is very important for reactor control and stability. Therefore, in this problem, we use neural network to model the relationship between the CB height and the power produced by the 22 fuel elements. The work by Dave et al. [75] explored the usage of machine learning methods such as gradient boosting and Gaussian process regression to generate empirical models for the MIT reactor. Therefore, we have used the proposed model of the MIT reactor developed by Dave et al. [75] to generate 1000 samples of different CB depths and their corresponding power levels of the 22 fuel elements. These samples are used to train a neural network model to control the reactor. In a separate study [76], the authors reported about 1%-2% noise in power signals coming from the reactor sensors. Therefore, to account for label noise during training, we added Gaussian noise to 350 samples (1/3 of the dataset) with the prescribed noise range. The network is then trained based on both clean and noisy data, while it is tested to predict clean data. Given the small value of the signal noise, it is unlikely this will have large impact on the training process.

The objective of this application is to *use NEORL to build the neural network such that the mean absolute error (MAE) in the test set can be as low as possible*. In other words, the optimized neural network will predict the reactor power globally, given the positions of the six CBs. According to this paper [77], for labelled data with small noise, classical regularization methods such as dropout or weight decay (L1, L2) is sufficient to ensure model robustness. We have

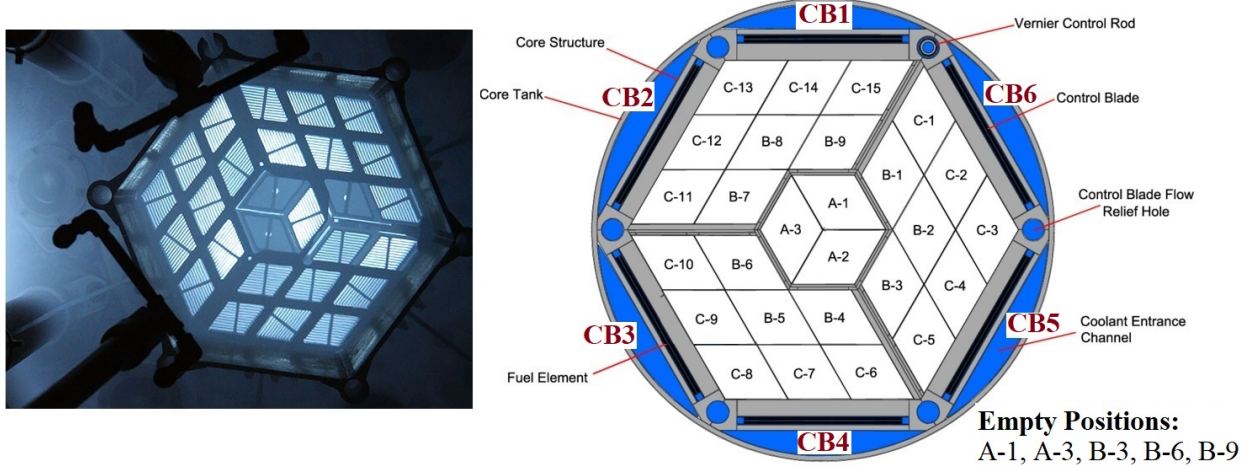


Figure 6: Top view of the MIT reactor core (Empty positions are used for experiments and do not have fuel)

used 800 samples for training (contain clean and noisy data) and 200 samples for testing (with clean data only). We formulate the optimization problem as follows

$$\min_{\vec{x}} f(\vec{x}) = \min_{\vec{x}} \text{MAE}(\vec{x}) = \frac{1}{N_{test}} \sum_{i=1}^{N_{test}} [\hat{y}(\vec{x}) - y]^2 \quad (23)$$

where $N_{test} = 200$ is the test set size, \hat{y} is the neural network prediction, and y is the target/real value from the test set. The input vector \vec{x} represents the features of the feedforward neural network to be optimized by NEORL, which are:

1. Number of hidden layers (Layers): A *discrete* variable in the range [2,7].
2. Learning rate (LR): A *continuous* variable in the range [1e-4,1e-3].
3. Batch size (Batch): A *categorical* variable from the list {8, 16, 32, 64, 128}.
4. Regularization for noise handling (Dropout): A *continuous* variable in the range [0,0.5] to improve network robustness against noisy labels.
5. Number of nodes in layer 1 (N_1): A *discrete* variable in the range [100,200].
6. Number of nodes in layer 2 (N_2): A *discrete* variable in the range [100,150].
7. Number of nodes in layer 3 if used from item 1 (N_3): A *discrete* variable in the range [100,150].
8. Number of nodes in layer 4 if used from item 1 (N_4): A *discrete* variable in the range [50,100].
9. Number of nodes in layer 5 if used from item 1 (N_5): A *discrete* variable in the range [50,100].
10. Number of nodes in layer 6 if used from item 1 (N_6): A *discrete* variable in the range [25,50].
11. Number of nodes in layer 7 if used from item 1 (N_7): A *discrete* variable in the range [25,50].

Therefore, this application is a NEORL demonstration of mixed discrete/categorical/continuous optimization. We used five different NEORL algorithms to solve this problem: HHO, PESA, BAT, ES, and GWO, which all can solve mixed optimization problems. All algorithms have been executed for 10 generations, 10 individuals per generation, leading to a total of 100 neural network architectures evaluated per algorithm. Table 6 lists the final results for all algorithms, which include the lowest MAE achieved and the optimized neural network variables corresponding to this MAE. We can notice very good agreement between the algorithms, especially between BAT and GWO, with four algorithms predicting with $\text{MAE} \leq 20$ Watt. All algorithms agree on the optimal network to be shallow with 2 hidden layers rather than being deep. In addition, all algorithms agree on batch size of 8, and on a minimal to zero dropout rate. This again confirms that the effect of the noise on the network performance is negligible such that dropout regularization is not needed. All tests have been executed using a workstation with 2 CPU nodes, 16 processors, 32 threads, 128 GB of memory, and GPU support.

In Table 7, we benchmark BAT, GWO, and PESA as the best NEORL algorithms to other algorithms from nlopt [51] and EvoloPy [26] in terms of lowest MAE and computing time. As indicated in Table 3, both nlopt and EvoloPy do

Table 6: Comparison of different neural network architectures for the MIT reactor as found by different NEORL optimizers

Method	Layers	LR	Batch	Dropout	N_1	N_2	N_3	N_4	N_5	N_6	N_7	MAE (Watt)
BAT	2	5.64E-04	8	0.00	148	147	0	0	0	0	0	17.2
GWO	2	6.71E-04	8	0.00	102	137	0	0	0	0	0	17.8
ES	2	5.33E-04	8	0.00	184	126	0	0	0	0	0	18.3
PESA	2	8.63E-04	8	0.00	101	122	0	0	0	0	0	19.9
HHO	2	3.41E-04	8	0.06	184	123	0	0	0	0	0	26.4

not support parallel optimization, thus these algorithms have been executed on a single processor for same amount of function evaluations as NEORL in Table 6. We can notice how much time saving NEORL can achieve in Table 7, as PESA (the fastest algorithm among all), can be 15 times faster compared to BOBYQA, and up to 18 times faster compared to sine cosine algorithm. Not only that, but also BAT and GWO are showing lower MAE results than other nlopt/EvolvoPy algorithms.

Table 7: Comparison of best NEORL algorithms against other frameworks for the MIT reactor neural network optimization

Algorithm (Framework)	MAE (Watt)	Computational Time (s)
Controlled Random Search (nlopt) [51]	19.0	912
Nelder Mead Simplex (nlopt) [51]	19.2	871
BOBYQA (nlopt) [51]	17.9	833
Firefly Algorithm (EvolvoPy) [26]	42.7	950
Multi-verse Optimizer (EvolvoPy) [26]	33.5	927
Since Cosine Algorithm (EvolvoPy) [26]	18.9	981
PESA (NEORL)	19.9	55*
GWO (NEORL)	17.8	95*
BAT (NEORL)	17.2	226*

* PESA, BAT, and GWO are running in parallel with 10 processors per algorithm.

4.3 Additional Applications

For brevity, we refer the reader to more NEORL applications available on the webpage⁴. We illustrate how RL algorithms can solve classical combinatorial problems such as travel salesman problem⁵ and knapsack problem⁶, while NEORL hyperparameter tuning tools help RL algorithms to achieve an optimal performance. In addition, we have demonstrated how variety of classical and modern evolutionary algorithms can be used to design a three-bar truss⁷, welded beam⁸, pressure vessel⁹, and others, which involve solving different problem types with different constraints. Our results in this work, which come from a single framework, show very competitive performance with the literature results that include a very diverse range of algorithms and implementations.

5 Conclusions

In this work, we have presented NEORL as an advanced optimization framework that features different computational capabilities to solve large-scale optimization problems along with a friendly interface. However, we should emphasize that the novelty of this work is not only framework development with demonstration on engineering applications, but more importantly on the algorithm methodology being developed. The ability to bring the state-of-the-art algorithms

⁴<https://neorl.readthedocs.io/en/latest/index.html>

⁵<https://neorl.readthedocs.io/en/latest/examples/ex1.html>

⁶<https://neorl.readthedocs.io/en/latest/examples/ex10.html>

⁷<https://neorl.readthedocs.io/en/latest/examples/ex6.html>

⁸<https://neorl.readthedocs.io/en/latest/examples/ex3.html>

⁹<https://neorl.readthedocs.io/en/latest/examples/ex8.html>

from neural networks, evolutionary computation, and neuroevolution in a cohesive environment is the core contribution of this work. Furthermore, some of these algorithms are actually proposed and developed by the authors.

Featuring +25 algorithms from different categories in NEORL is vital to accommodate the “No Free Lunch Theorems for Optimization” [78], which state that “for any optimization algorithm, any elevated performance over one class of problems is offset by performance over another class”, which would imply that any optimization algorithm performance averaged over all possible problems will be close to random search. Therefore, providing the ability to deploy variety of algorithms with different natures from neural, evolutionary, and neuroevolution categories on the same problem, can provide the analyst of more comprehensive results than relying on a single algorithm.

In conclusion, solving optimization problems is at the heart of many disciplines to find the most optimal solutions to their problems, which require advanced algorithms and friendly framework implementation. In this work, we proposed and benchmarked NEORL, which is a framework for NeuroEvolution Optimization with Reinforcement Learning. NEORL was developed with a main purpose to resolve the issues facing other Python optimization frameworks by providing an interface of state-of-the-art algorithms in the field of evolutionary computation, neural networks, reinforcement learning, and hybrid neuroevolution algorithms. The novelty of NEORL originates from the diversity of the implemented algorithms, advanced implementation, user-friendly interface, parallel computing support, hyperparameter tuning, detailed documentation, and demonstration of applications in mathematical and real-world engineering optimization. NEORL was benchmarked against many algorithms from the literature and against other popular optimization frameworks (nlopt, EvoloPy, DEAP, PyOpt); showing an excellent and competitive performance.

Future steps of NEORL will focus on two major paths. First, we will add special algorithms and capabilities for direct multi-objective optimization if the user prefers to avoid using priori conversion methods. Second, more advanced applications will be pursued by the authors, in which NEORL is utilized directly to solve large-scale design problems with more problem-dependent physics guidance, which can be obtained in form of sensitivity coefficients [79, 80] or data-driven physical closures [81]. Given its open-source nature, the authors also welcome contributions from researchers around the world who are willing to enrich NEORL family with new algorithms and/or applications.

6 Data Availability

NEORL framework is open-source, and it can be accessed from: <https://github.com/mradaideh/neorl>. The documentation and tutorials are available here: <https://neorl.readthedocs.io/en/latest/index.html>.

All scripts used in this paper can be found under the `examples` directory within NEORL: https://github.com/mradaideh/neorl/tree/master/examples/journal_tests.

Acknowledgment

This work is sponsored by Exelon Corporation, a nuclear electric power generation company, under the award (40008739). The authors would like to thank Benoit Forget of Massachusetts Institute of Technology (MIT), Isaac Wolverton and Joshua Joseph of MIT Quest for Intelligence, and James J. Tusar and Ugi Otgonbaatar of Exelon corporation, for their feedback and discussions in the early phase of the project.

Credit Author Statement

Majdi I. Radaideh: Conceptualization, Methodology, Software, Validation, Investigation, Data curation, Visualisation, Formal analysis, Writing - Original Draft.

Katelin Du: Methodology, Software, Validation, Formal analysis, Writing - Original Draft.

Paul Seurin: Methodology, Software, Validation, Formal analysis, Writing - Original Draft.

Devin Seyler: Methodology, Software, Validation, Formal analysis, Writing - Original Draft.

Xubo Gu: Methodology, Software, Writing – Review and Edit.

Haijia Wang: Methodology, Software, Writing – Review and Edit.

Koroush Shirvan: Conceptualization, Methodology, Funding acquisition, Resources, Writing – Review and Edit.

References

- [1] R. H. Stewart, T. S. Palmer, B. DuPont, A survey of multi-objective optimization methods and their applications for nuclear scientists and engineers, Progress in Nuclear Energy (2021) 103830.

- [2] S. P. Rajput, S. Datta, A review on optimization techniques used in civil engineering material and structure design, *Materials Today: Proceedings* 26 (2020) 1482–1491.
- [3] K. P. Bennett, E. Parrado-Hernández, The interplay of optimization and machine learning research, *The Journal of Machine Learning Research* 7 (2006) 1265–1281.
- [4] A. Soler-Dominguez, A. A. Juan, R. Kizys, A survey on financial applications of metaheuristics, *ACM Computing Surveys (CSUR)* 50 (1) (2017) 1–23.
- [5] A. Ahmadi-Javid, Z. Jalali, K. J. Klassen, Outpatient appointment systems in healthcare: A review of optimization studies, *European Journal of Operational Research* 258 (1) (2017) 3–34.
- [6] S. Sivanandam, S. Deepa, Genetic algorithms, in: *Introduction to genetic algorithms*, Springer, 2008, pp. 15–37.
- [7] T. Glasmachers, T. Schaul, S. Yi, D. Wierstra, J. Schmidhuber, Exponential natural evolution strategies, in: *Proceedings of the 12th annual conference on Genetic and evolutionary computation*, 2010, pp. 393–400.
- [8] N. Hansen, The cma evolution strategy: a comparing review, *Towards a new evolutionary computation* (2006) 75–102.
- [9] T. Salimans, J. Ho, X. Chen, S. Sidor, I. Sutskever, Evolution strategies as a scalable alternative to reinforcement learning, *arXiv preprint arXiv:1703.03864*.
- [10] J. Kennedy, R. Eberhart, Particle swarm optimization, in: *Proceedings of ICNN'95-international conference on neural networks*, Vol. 4, IEEE, 1995, pp. 1942–1948.
- [11] R. Storn, K. Price, Differential evolution—a simple and efficient heuristic for global optimization over continuous spaces, *Journal of global optimization* 11 (4) (1997) 341–359.
- [12] M. Dorigo, G. Di Caro, Ant colony optimization: a new meta-heuristic, in: *Proceedings of the 1999 congress on evolutionary computation-CEC99 (Cat. No. 99TH8406)*, Vol. 2, IEEE, 1999, pp. 1470–1477.
- [13] F. Glover, Tabu search—part i, *ORSA Journal on computing* 1 (3) (1989) 190–206.
- [14] D. Karaboga, B. Basturk, A powerful and efficient algorithm for numerical function optimization: artificial bee colony (abc) algorithm, *Journal of global optimization* 39 (3) (2007) 459–471.
- [15] X.-S. Yang, S. Deb, Cuckoo search via lévy flights, in: *2009 World congress on nature & biologically inspired computing (NaBIC)*, Ieee, 2009, pp. 210–214.
- [16] X.-S. Yang, A new metaheuristic bat-inspired algorithm, in: *Nature inspired cooperative strategies for optimization (NISCO 2010)*, Springer, 2010, pp. 65–74.
- [17] S. Mirjalili, S. M. Mirjalili, A. Lewis, Grey wolf optimizer, *Advances in engineering software* 69 (2014) 46–61.
- [18] S. Mirjalili, A. Lewis, The whale optimization algorithm, *Advances in engineering software* 95 (2016) 51–67.
- [19] S. Mirjalili, Moth-flame optimization algorithm: A novel nature-inspired heuristic paradigm, *Knowledge-based systems* 89 (2015) 228–249.
- [20] S. Mirjalili, A. H. Gandomi, S. Z. Mirjalili, S. Saremi, H. Faris, S. M. Mirjalili, Salp swarm algorithm: A bio-inspired optimizer for engineering design problems, *Advances in Engineering Software* 114 (2017) 163–191.
- [21] A. A. Heidari, S. Mirjalili, H. Faris, I. Aljarah, M. Mafarja, H. Chen, Harris hawks optimization: Algorithm and applications, *Future generation computer systems* 97 (2019) 849–872.
- [22] A. Slowik, H. Kwasnicka, Evolutionary algorithms and their applications to engineering problems, *Neural Computing and Applications* (2020) 1–17.
- [23] S. Mirjalili, J. S. Dong, A. Lewis, *Nature-inspired optimizers: theories, literature reviews and applications*, Vol. 811, Springer, 2019.
- [24] H. Faris, I. Aljarah, M. A. Al-Betar, S. Mirjalili, Grey wolf optimizer: a review of recent variants and applications, *Neural computing and applications* 30 (2) (2018) 413–435.
- [25] F.-A. Fortin, F.-M. De Rainville, M.-A. Gardner, M. Parizeau, C. Gagné, DEAP: Evolutionary algorithms made easy, *Journal of Machine Learning Research* 13 (2012) 2171–2175.
- [26] H. Faris, I. Aljarah, S. Mirjalili, P. A. Castillo, J. J. M. Guervós, Evolopy: An open-source nature-inspired optimization framework in python., in: *IJCCI (ECTA)*, 2016, pp. 171–177.
- [27] J. Schmidhuber, Deep learning in neural networks: An overview, *Neural networks* 61 (2015) 85–117.
- [28] G. Joya, M. Atencia, F. Sandoval, Hopfield neural networks for optimization: study of the different dynamics, *Neurocomputing* 43 (1-4) (2002) 219–237.
- [29] O. Vinyals, M. Fortunato, N. Jaitly, Pointer networks, *arXiv preprint arXiv:1506.03134*.
- [30] V. Mnih, K. Kavukcuoglu, D. Silver, A. A. Rusu, J. Veness, M. G. Bellemare, A. Graves, M. Riedmiller, A. K. Fidjeland, G. Ostrovski, et al., Human-level control through deep reinforcement learning, *nature* 518 (7540) (2015) 529–533.
- [31] K. Li, J. Malik, Learning to optimize, *arXiv preprint arXiv:1606.01885*.

- [32] I. Bello, H. Pham, Q. V. Le, M. Norouzi, S. Bengio, Neural combinatorial optimization with reinforcement learning, arXiv preprint arXiv:1611.09940.
- [33] E. Khalil, H. Dai, Y. Zhang, B. Dilkina, L. Song, Learning combinatorial optimization algorithms over graphs, in: *Advances in Neural Information Processing Systems*, 2017, pp. 6348–6358.
- [34] M. I. Radaideh, I. Wolverson, J. Joseph, J. J. Tusar, U. Otgonbaatar, N. Roy, B. Forget, K. Shirvan, Physics-informed reinforcement learning optimization of nuclear assembly design, *Nuclear Engineering and Design* 372 (2021) 110966.
- [35] Machine learning for combinatorial optimization: A methodological tour d’horizon, *European Journal of Operational Research* 290 (2) (2021) 405–421.
- [36] P. Dhariwal, C. Hesse, O. Klimov, A. Nichol, M. Plappert, A. Radford, J. Schulman, S. Sidor, Y. Wu, P. Zhokhov, Openai baselines, <https://github.com/openai/baselines> (2017).
- [37] A. Hill, A. Raffin, M. Ernestus, A. Gleave, A. Kanervisto, R. Traore, P. Dhariwal, C. Hesse, O. Klimov, A. Nichol, M. Plappert, A. Radford, J. Schulman, S. Sidor, Y. Wu, Stable baselines, <https://github.com/hill-a/stable-baselines> (2018).
- [38] K. O. Stanley, R. Miikkulainen, Evolving neural networks through augmenting topologies, *Evolutionary computation* 10 (2) (2002) 99–127.
- [39] K. O. Stanley, D. B. D’Ambrosio, J. Gauci, A hypercube-based encoding for evolving large-scale neural networks, *Artificial life* 15 (2) (2009) 185–212.
- [40] F. P. Such, V. Madhavan, E. Conti, J. Lehman, K. O. Stanley, J. Clune, Deep neuroevolution: Genetic algorithms are a competitive alternative for training deep neural networks for reinforcement learning, arXiv preprint arXiv:1712.06567.
- [41] B. Zhao, F. Luo, H. Lin, D. Liu, Particle swarm optimized neural networks based local tracking control scheme of unknown nonlinear interconnected systems, *Neural Networks* 134 (2021) 54–63.
- [42] J. Jiang, F. Han, Q. Ling, J. Wang, T. Li, H. Han, Efficient network architecture search via multiobjective particle swarm optimization based on decomposition, *Neural Networks* 123 (2020) 305–316.
- [43] J. E. Pettinger, R. M. Everson, Controlling genetic algorithms with reinforcement learning, in: *Proceedings of the 4th Annual Conference on Genetic and Evolutionary Computation*, 2002, pp. 692–692.
- [44] M. I. Radaideh, K. Shirvan, Rule-based reinforcement learning methodology to inform evolutionary algorithms for constrained optimization of engineering applications, *Knowledge-Based Systems* 217 (2021) 106836.
- [45] D. E. Moriarty, A. C. Schultz, J. J. Grefenstette, Evolutionary algorithms for reinforcement learning, *Journal of Artificial Intelligence Research* 11 (1999) 241–276.
- [46] M. M. Drugan, Reinforcement learning versus evolutionary computation: A survey on hybrid algorithms, *Swarm and evolutionary computation* 44 (2019) 228–246.
- [47] Y. Tenne, C.-K. Goh, *Computational intelligence in expensive optimization problems*, Vol. 2, Springer Science & Business Media, 2010.
- [48] A. I. Forrester, A. J. Keane, Recent advances in surrogate-based optimization, *Progress in aerospace sciences* 45 (1-3) (2009) 50–79.
- [49] Y. Jin, M. Olhofer, B. Sendhoff, A framework for evolutionary optimization with approximate fitness functions, *IEEE Transactions on evolutionary computation* 6 (5) (2002) 481–494.
- [50] G. Briffoteaux, M. Gobert, R. Ragonnet, J. Gmys, M. Mezmez, N. Melab, D. Tuytens, Parallel surrogate-assisted optimization: Batched bayesian neural network-assisted ga versus q-ego, *Swarm and Evolutionary Computation* 57 (2020) 100717.
- [51] S. G. Johnson, The nlopt nonlinear-optimization package, <http://github.com/stevengj/nlopt> (2014).
- [52] R. E. Perez, P. W. Jansen, J. R. Martins, pyopt: a python-based object-oriented framework for nonlinear constrained optimization, *Structural and Multidisciplinary Optimization* 45 (1) (2012) 101–118.
- [53] P. Virtanen, R. Gommers, T. E. Oliphant, M. Haberland, T. Reddy, D. Cournapeau, E. Burovski, P. Peterson, W. Weckesser, J. Bright, et al., Scipy 1.0: fundamental algorithms for scientific computing in python, *Nature methods* 17 (3) (2020) 261–272.
- [54] J. Schulman, P. Moritz, S. Levine, M. Jordan, P. Abbeel, High-dimensional continuous control using generalized advantage estimation, arXiv preprint arXiv:1506.02438.
- [55] M. I. Radaideh, B. Forget, K. Shirvan, Large-scale design optimisation of boiling water reactor bundles with neuroevolution, *Annals of Nuclear Energy* 160 (2021) 108355.
- [56] M. I. Radaideh, K. Shirvan, Improving intelligence of evolutionary algorithms using experience share and replay, arXiv preprint arXiv:2009.08936.
- [57] T. Schaul, J. Quan, I. Antonoglou, D. Silver, Prioritized experience replay, arXiv preprint arXiv:1511.05952.
- [58] P. Huang, H. Wang, Y. Jin, Offline data-driven evolutionary optimization based on tri-training, *Swarm and Evolutionary Computation* 60 (2021) 100800.
- [59] Y. Cui, Z. Geng, Q. Zhu, Y. Han, Multi-objective optimization methods and application in energy saving, *Energy* 125 (2017) 681–704.

- [60] O. Kramer, A review of constraint-handling techniques for evolution strategies, *Applied Computational Intelligence and Soft Computing* 2010.
- [61] C. A. C. Coello, Use of a self-adaptive penalty approach for engineering optimization problems, *Computers in Industry* 41 (2) (2000) 113–127.
- [62] M. Ni, M. K. Leung, D. Y. Leung, Parametric study of solid oxide fuel cell performance, *Energy Conversion and Management* 48 (5) (2007) 1525–1535.
- [63] H. Zhang, H. Xu, B. Chen, F. Dong, M. Ni, Two-stage thermoelectric generators for waste heat recovery from solid oxide fuel cells, *Energy* 132 (2017) 280–288.
- [64] M. İnci, A. Caliskan, Performance enhancement of energy extraction capability for fuel cell implementations with improved cuckoo search algorithm, *International Journal of Hydrogen Energy* 45 (19) (2020) 11309–11320.
- [65] V. Kannan, H. Xue, K. A. Raman, J. Chen, A. Fisher, E. Birgersson, Quantifying operating uncertainties of a pemfc–monte carlo-machine learning based approach, *Renewable Energy* 158 (2020) 343–359.
- [66] P. Mojaver, S. Khalilarya, A. Chitsaz, Combined systems based on osofc/hsofc: Comparative analysis and multi-objective optimization of power and emission, *International Journal of Energy Research* 45 (4) (2021) 5449–5469.
- [67] M. I. Radaideh, M. I. Radaideh, T. Kozłowski, Design optimization under uncertainty of hybrid fuel cell energy systems for power generation and cooling purposes, *International Journal of Hydrogen Energy* 45 (3) (2020) 2224–2243.
- [68] M. I. Radaideh, M. I. Radaideh, Efficient analysis of parametric sensitivity and uncertainty of fuel cell models with application to sofc, *International Journal of Energy Research* 44 (4) (2020) 2517–2534.
- [69] H. Zhang, J. Chen, J. Zhang, Performance analysis and parametric study of a solid oxide fuel cell fueled by carbon monoxide, *International Journal of Hydrogen Energy* 38 (36) (2013) 16354–16364.
- [70] M. El-Sefy, A. Yosri, W. El-Dakhkhni, S. Nagasaki, L. Wiebe, Artificial neural network for predicting nuclear power plant dynamic behaviors, *Nuclear Engineering and Technology*.
- [71] J. Bae, G. Kim, S. J. Lee, Real-time prediction of nuclear power plant parameter trends following operator actions, *Expert Systems with Applications* (2021) 115848.
- [72] Y. Liu, N. Dinh, Y. Sato, B. Niceno, Data-driven modeling for boiling heat transfer: using deep neural networks and high-fidelity simulation results, *Applied Thermal Engineering* 144 (2018) 305–320.
- [73] M. I. Radaideh, T. Kozłowski, Combining simulations and data with deep learning and uncertainty quantification for advanced energy modeling, *International Journal of Energy Research* 43 (14) (2019) 7866–7890.
- [74] Y. Liu, D. Wang, X. Sun, N. Dinh, R. Hu, Uncertainty quantification for multiphase-cfd simulations of bubbly flows: a machine learning-based bayesian approach supported by high-resolution experiments, *Reliability Engineering & System Safety* 212 (2021) 107636.
- [75] A. J. Dave, J. Yu, J. Wilson, B. Phillips, K. Sun, B. Forget, Empirical models for multidimensional regression of fission systems, *arXiv preprint arXiv:2105.14645*.
- [76] A. J. Dave, K. Sun, L.-w. Hu, S. H. Pham, E. H. Wilson, D. Jaluvka, Thermal-hydraulic analyses of mit reactor leu transition cycles, *Progress in Nuclear Energy* 118 (2020) 103117.
- [77] H. Song, M. Kim, D. Park, Y. Shin, J.-G. Lee, Learning from noisy labels with deep neural networks: A survey, *arXiv preprint arXiv:2007.08199*.
- [78] D. H. Wolpert, W. G. Macready, No free lunch theorems for optimization, *IEEE transactions on evolutionary computation* 1 (1) (1997) 67–82.
- [79] K. Borowiec, T. Kozłowski, C. S. Brooks, Validation and uncertainty quantification for two-phase natural circulation flows using trace code, *Nuclear Science and Engineering* 194 (8-9) (2020) 737–747.
- [80] D. Price, A. Maile, J. Peterson-Droogh, D. Blight, A methodology for uncertainty quantification and sensitivity analysis for responses subject to monte carlo uncertainty with application to fuel plate characteristics in the atrc, *Nuclear Engineering and Technology*.
- [81] K. Borowiec, A. J. Wysocki, T. Kozłowski, Comprehensive framework for data-driven model form discovery of the closure laws in thermal-hydraulics codes, *International Journal of Heat and Mass Transfer* 170 (2021) 120976.